WILEY Journal of Applied Polymer Science

On the use of TNPP as chain extender in melt blended PHBV/clay nanocomposites: morphology, thermal stability and mechanical properties

Journal:	*Journal of Applied Polymer Science*
Manuscript ID:	APP-2015-01-0233
Wiley - Manuscript type:	Research Article
Keywords:	Biopolymers & renewable polymers, clay, nanoparticles, nanowires and nanocrystals, thermogravimetric analysis (TGA)

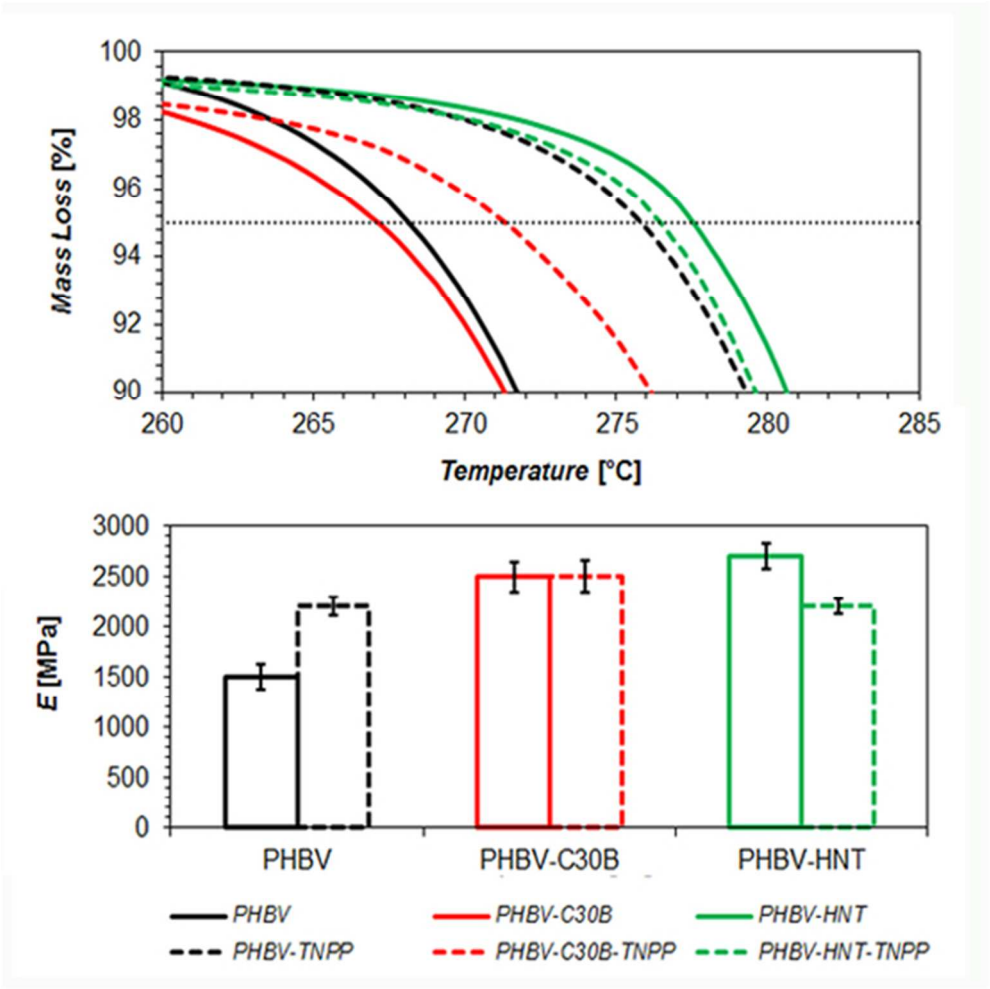

50x50mm (300 x 300 DPI)

On the use of TNPP as a chain extender in melt blended PHBV/clay nanocomposites: morphology, thermal stability, and mechanical properties.

Jennifer González-Ausejo,[1] Estefania Sánchez-Safont,[1] José Gámez-Pérez,[1] Luis Cabedo[1*]

[1] Polymer and Advanced Materials Group (PIMA), Universidad Jaume I, 12071, Castellon, Spain.

* Correspondence to: Luis Cabedo (E-mail: *lcabedo@uji.es*)

ABSTRACT

The influence of the incorporation of tris(nonylphenyl) phosphite (TNPP) as a chain extender on the morphology and thermal stability of poly(hydroxybutyrate-co-hydroxyvalerate) (PHBV)/clay nanocomposites obtained by melt mixing has been studied. Two different clays have been used: a laminar organomodified montmorillonite (Cloisite® 30B) and a tubular unmodified halloysite (HNT). The morphology of the so-obtained nanocomposites has been assessed by TEM, SEM, and WAXS, showing a partially exfoliated structure for PHBV/Cloisite® 30B nanocomposites, as well as a good dispersion of the HNT in the PHBV matrix. The crystallinity of the resulting nanocomposites has been determined by DSC, showing a nucleating effect of both nanoclays on the PHBV matrix. An increase in the onset temperature of thermal degradation of PHBV has been obtained with the addition of TNPP, as determined by TGA. With regard to the effect of the nanoclays on the thermal stability of PHBV, the onset temperature of the PHBV/HNT nanocomposites is higher than that of the pure PHBV, while this trend is not observed for the nanocomposites containing Cloisite® 30B. The addition of TNPP to the PHBV/Cloisite® 30B nanocomposites resulted in an improved thermal stability; however, for the HNT nanocomposites, the TNPP does not seem to have a significant effect. For all studied systems, it was shown that the variation of mechanical properties of these nanocomposites is strongly influenced by their changes in crystallinity and in the case of TNPP addition it is due to the increased molecular weight and formation of a long chain branching structure.

KEYWORDS

PHBV, halloysite, organomodified montmorillonite, chain extenders, thermal stability, melt blending.

INTRODUCTION

Poly(hydroxybutyrate-co-hydroxyvalerate) (PHBV), a biodegradable copolyester from the polyhydroxyalkanoate family (PHA), has gained a lot of attention because of its fast biodegradability and biocompatibility as well as a non-food-competitive origin [1]. Particularly in the packaging field, PHBV has shown a great interest because its inertness and chemical stability that makes it suitable for applications as films for food contact material with any type of food [2]. It has been suggested, as a matter of fact, that PHBV could replace polypropylene [3] or poly(ethylene terephtalate) [4] in many applications in where it would not be necessary to modify their processing. In spite of the significant potential of PHBV to substitute for commodity polymers, it still presents a number of property and processing shortcomings that handicap its use in many applications. [5] When compared to other linear polymers, PHBV has shown lower mechanical and gas barrier properties, as well as lower thermal resistance during processing. [4,6]

Nanotechnology brings significant opportunities to improve the applicability of PHBV to the food packaging field. [5,7] The increase in mechanical properties of biopolymers by incorporating low amounts of nanoparticles has been widely reported.[6,8,9] Indeed, some works have shown that the use of nanocomposites in food packaging applications, when properly prepared, is harmless and free potential migration issues. [7] The obtaining of polymer nanocomposites has been reported to be a promising way to improve the barrier properties against gases, aromas, and water vapor. Some reported nanofillers are carbon nanotubes, nanoclays and halloysite nanotubes, among others. [6,10]

The montmorillonite is the most commonly used nanoclay in the field of polymer nanocomposites. [8] It is a natural clay belonging to the family of 2:1 layered silicates, also

called 2:1 phyllosilicates. Its structure consists of layers made up of two tetrahedrally coordinated silicon atoms bonded to an edge-shared octahedral sheet of either aluminum or magnesium hydroxide. This nanoclay requires surface modification (organomodification) to achieve a good degree of delamination when mixed with polymers. The chemicals more widely used for organomodification of montmorillonites are alkylammonium cations. Studies have shown that the reduction in permeability of polymer/clay nanocomposites is based on an increase in the tortuosity of the diffusion path taken by small molecules.[6,8–11] The effect of nanoclays on the properties of the polymer matrix is highly dependent on the degree of dispersion achieved during mixing [9]; hence sometimes surface modification of the nanoclays is required in order to increase their compatibility. In the case of PHBV nanocomposites, the use of organomodified clays containing surfactants appears to be a suitable way to improve their affinity to the polymer and dispersion within the matrix.[12–14] However, the addition of organomodified clays can lead to higher polymer degradation during melt processing,[12–14] due to a catalytic effect of their decomposition products.[14–16]

Recently, halloysite nanotubes (HNTs) have attracted interest as nanoparticles for biopolymers because they are economical and abundantly available and have rich functionality, good biocompatibility, and high mechanical strength. [17] Halloysite belongs to the kaolin group of clay minerals. It exhibits a predominantly hollow tubular structure in the nanoscale range and a large aspect ratio. [18] The surface of HNTs is comprised of siloxane and hydroxyl groups, which gives halloysites potential for the formation of hydrogen bonds and hence improves the dispersion in some polymer matrixes without any chemical modification, especially when compared to other two-dimensional nanoclay fillers such as montmorillonites.[19,20] Moreover, the higher stiffness of the HNTs compared to

montmorillonite platelets and the high length-to-diameter aspect ratio of the tubes can promote excellent nano-reinforcement for polymer nanocomposites.[12,20–22]

As mentioned before, the degradation of biopolyesters, more specifically PHBV, during processing in molten conditions is a factor that inevitably limits the range of applications.[23] The use of chain extenders is a convenient approach for improving the thermal stability of biopolyesters during processing. [24–33] The chain extension is a reaction that avoids a drop in molecular weight. The reaction between carboxylic end groups on polyesters and the functional groups of chain extenders, such as hydroxyl, amine, anhydride, epoxy, or carboxylic acid, are the key reactions for improving thermal resistance.[34] This approach has been successfully applied to blends from several matrices like Poly(lactic acid) (PLA), poly(butylene adipate-co-terephthalate) (PBAT), Polybutylene succinate (PBS), and Polybutylene terephthalate (PBT) with chain extenders such as Joncryl® ADR,[24–28] dicumyl peroxide (DCP),[29] hexamethylene diisocyanate (HDI),[28] pyromellitic dianhydride (PDMA),[28] tris(nonylphenyl)phosphite (TNPP),[24,25,30–32] and polycarbodiimide (PCDI).[24,25]

Some studies have developed the use of DCP[35,36] or Joncryl® ADR-4368[37] in PHBV. Haene et al.[35] studied the branching behavior of PHBV using low levels of DCP, reporting a branching process of PHBV observed from the increase in strain hardening with the addition of higher concentrations of DCP. Fei et al.[36] studied the cross-linking of PHBV using a high level of DCP and observed enhanced melt viscosity and mechanical properties without compromising the biodegradability. On the other hand, Duangphet et al.[37] studied the effect of an epoxy-functionalized chain extender (Joncryl® ADR-4368 S) on degradation during melt blending of PHBV conducted in a twin screw extruder, showing an improvement in the resistance to thermal decomposition of PHBV, an enhancement of PHBV melt viscosity, and also a

reduction of the crystallization rate by introducing the chain extender due to the increase in molecular weight and chain rigidity.

The use of chain extenders in the production of polymer-based nanocomposites has been studied.[24–26,28] Najafi et al.[24–26] and Meng et al.[28] studied the effect of clay (Cloisite 30B) and different chain extenders [PCDI, TNPP, pyromellitic dianhydride (PMDA), hexamethylene diisocyanate (HDI), and Joncryl® ADR 4368] on the thermal degradation, morphology, and crystallization behavior of PLA. According to Najafi et al., the incorporation of a chain extender into the nanocomposites had a profound effect on controlling the degradation and also increasing the molecular weight, resulting in an increase of the polymer viscosity.[24–26] Also, Meng et al. found that the chain extenders have a remarkable stabilization effect on PLA/clay nanocomposites without negatively affecting the clay dispersion.[28]

Tris(nonylphenyl) phosphite (TNPP) has been successfully used as chain extender in other matrices[30–32] leading to thermal stabilization with low contents. Indeed, TNPP is characterized by being suitable for food contact[38], thus being suitable for food packaging applications. Burlett et al.[30] reported that the stabilizing effect of TNPP was strongly dependent on the concentration used. Cicero et al.[31] showed that the molecular weight of extrusion-processed PLA may be stabilized by adding less than 1 wt% of TNPP prior to extrusion and reported an improvement of the mechanical properties with such an addition. Lehermeier et al.[32] reported that the addition of 0.35 wt% of TNPP provides excellent stabilization over a range of temperatures. However, to the best of our knowledge, its effect in PHBV has never been studied.

Within this context, the aim of this study was to evaluate the effect of the addition of TNPP as a chain extender with two types of clays (Cloisite® 30B and halloysite nanotubes) on the

morphology, thermal and mechanical properties of PHBV nanocomposites for food packaging applications.

EXPERIMENTAL

Materials

Poly(hydroxybutyrate-co-hydroxyvalerate) (PHBV) with 3 mol% hydroxyvalerate content was purchased from Tianan Biologic Material Co. (Ningbo, P.R. China) in pellet form (ENMAT Y1000P). Two different commercial nanoclays were used in this study: organomodified montmorillonite Cloisite® 30B (hereafter referred to as C30B) containing a methyl bis-2-hydroxyethyl ammonium quaternary salt, supplied by Southern Clay Products; and halloysite (HNT), an unmodified tubular clay from NaturalNano Inc. The chain extender used was tris(nonylphenyl) phosphite (TNNP) supplied by Sigma Aldrich.

Nanocomposite preparation

PHBV and the clays used in this study were dried under vacuum at 80 °C for 2 h before use, while the chain extender was used as received. The PHBV blends and nanocomposites were obtained by melt blending using an internal mixer (Rheomix 3000P ThermoHaake, Karlsruhe, Germany) during a mixing time of less than 6 minutes at a temperature of 180 °C and rotor speed of 100 rpm. The melt temperature was never allowed to reach 195 °C in order to avoid severe thermal degradation during blending. Plates (0.8 mm thick) and films (0.1 mm thick) were obtained from the blends in a hot-plate press at 185 °C and 3 bar for 3 min. Plates were used for morphological and thermal characterization, while films were used for the mechanical characterization. All the samples were stored in a vacuum desiccator at ambient temperature during two weeks to allow full crystallization to take place.[39–41]

Samples of both PHBV (referred to as neat PHBV) and PHBV with 1 wt% TNPP (PHBV-TNPP) were processed. The nomenclature used for the nanocomposites is as follows: PHBV-C30B and PHBV-HNT for the systems containing 5 wt% of Cloisite 30B and halloysite nanotubes, respectively, and PHBV-C30B-TNPP and PHBV-HNT-TNPP for the systems containing 5 wt% of Cloisite 30B and halloysite nanotubes together with 1 wt% TNPP as a chain extender.

Characterization

Transmission electron microscopy (TEM) of the nanocomposites was performed using a Jeol 2100 operated at 200 kV. The ultrathin sections with a thickness of 80 nm were prepared at room temperature using an RMC ultramicrotome (Model Powertome XL). The so-obtained films were placed on a carbon-coated copper grid for observation.

The morphology of the cryofractured surface of PHBV nanocomposites was evaluated by Scanning Electron Microscopy (SEM) using a JEOL 7001F. The samples were fractured in liquid nitrogen and subsequently coated by sputtering with a thin layer of Pt.

Wide angle X-ray diffraction (WAXD) measurements were performed using a Bruker AXS D4 Endeavour diffractometer. The samples were scanned at room temperature in reflection mode using incident Cu Ka radiation (k = 1.54 Å), while the generator was set up at 40 kV and 40 mA. The data were collected over a range of scattering angles (2θ) of 2–30°. The basal spacing (d-spacing) of the clays was estimated from the (001) diffraction peak using Bragg's law:

$$\lambda = 2 \cdot d \cdot sin\theta \quad (1)$$

The thermal stability of the nanocomposites was investigated by means of thermogravimetric analysis (TGA) using a TG-STDA Mettler Toledo model TGA/

SDTA851e/LF/1600. The samples were heated from 50 to 900 °C at a heating rate of 10 °C/min under nitrogen flow. The characteristic temperatures $T_{5\%}$ and T_d corresponded, respectively, to the initial decomposition temperature (5% of degradation) and to the maximum degradation rate temperature measured at the DTG peak maximum.

Differential scanning calorimeter (DSC) experiments were conducted using a PerkinElmer DSC-7. The weight of the DSC samples was typically 6 mg. Samples were first heated from 45 to 200 °C at 40 °C/min, kept for 1 min at 200 °C, cooled down to 45 °C at 10 °C/min, and then finally heated to 200 °C at 10 °C/min. The crystallization temperature (T_c), melt temperature (T_m), and melting enthalpy (ΔH_m) were determined from the cooling and second heating curve. T_m and ΔH_m were taken as the peak temperature and the area of the melting endotherm, respectively. The crystallinity (Xc) of the PHBV phase was calculated by the following expression:

$$X_c\ (\%) = \frac{\Delta H_m}{w \cdot \Delta H_m^0} \cdot 100 \qquad (2)$$

where ΔH_m (J/g) is the melting enthalpy of the polymer matrix, ΔH_m^0 is the melting enthalpy of 100% crystalline PHBV (perfect crystal) (146 J/g), and w is the polymer weight fraction of PHBV in the blend.[9] The DSC instrument was calibrated with an indium standard before use.

Tensile properties were measured in a universal testing machine (Instron 4469) at a crosshead speed of 10 mm/min and room temperature. All samples were conditioned under ambient conditions (25 °C and 50% R.H. for 24 hours). Tests were carried out according to ASTM D638 using films of approximately 100-μm thickness prepared by hot press. Five

specimens of each sample were tested and the average results with standard deviation were reported.

RESULTS AND DISCUSSION

Morphology

The morphology of the PHBV nanocomposites was evaluated by means of SEM, TEM, and WAXS. Figsures 1a and 1b present the TEM micrographs of the PHBV nanocomposites with 5 wt% of C30B and HNT, respectively. As seen in Fig. 1a, the presence of small intercalated structures with a large aspect ratio (tactoids) in the PHBV-C30B is observed. Nevertheless, the nanocomposites show a good dispersion of the montmorillonite platelets, also indicating that a high degree of delamination of the clay during melt processing was achieved.

The TEM micrograph of the PHBV-HNT sample (Fig. 1b) shows the presence of isolated nanotubes. In this figure, it is possible to identify a parallel-oriented nanotube showing the internal structure of the halloysite, which can be described as a hollow tubular morphology produced by the stacking of the clay mineral layers. From the TEM pictures, the dimensions of the halloysite tubes could be estimated: a length below 1 μm and external and internal nanotube diameters of 70 and 25 nm, respectively.

SEM micrographs of PHBV nanocomposites with and without TNPP are presented in Fig. 2. In the case of montmorillonite nanocomposites (Figs. 2a and 2b), a strong adhesion between the clay and the polymer matrix can be deduced from the look of the platelets, covered with the polymer matrix. In these figures it is possible to observe the presence of individual platelets (indicated with an arrow), as well as a good dispersion, in agreement with the TEM micrographs. Hence, it can be inferred that an effective mixing has been achieved.

The SEM micrographs of PHBV-HNT nanocomposites present a uniform dispersion of the halloysite nanotubes in both cases (with and without TNPP), shown as white dots in Fig. 2c and 2d. These micrographs are in agreement with TEM observations. However, different surface interaction between the halloysite and the PHBV can be observed depending on the presence of the chain extender. The sample without TNPP exhibits a good degree of adhesion of the polymer matrix on the nanoclay surface. On the other hand, the sample containing TNPP shows a slight detachment of the nanotubes from the polymer matrix. A possible explanation for this behavior is that the TNPP is partially absorbed on the surface of the nanotubes, thus leading to a decrease in the interaction between the nanoclay surface and the polymer matrix.

The WAXS diffractograms of the clays and PHBV nanocomposites are shown in Fig. 3. The PHBV diffractogram presents three main peaks at 2θ values of 13, 17, and 26. The first two peaks can be associated with the (020) and (110) reflections of the orthorhombic lattice of the PHBV respectively. The most intense peak at 2θ = 26 corresponds to the (002) reflexion of the boron nitride, which is present as a nucleating agent in the commercial grade used in this work. No noticeable difference in the peak positions and relative intensities can be observed when the clays or the TNPP are introduced; therefore, it can be concluded that the crystalline form of the PHBV is not affected by the addition of these nanoclays or the chain extender.

The diffraction pattern of C30B exhibits a peak at 2θ = 5°, corresponding to a basal spacing (001) of 1.76 nm according to the Bragg equation. The PHBV-C30B diffractogram shows the peak associated with the basal reflection of the C30B, which suggests that fully exfoliated morphology has not been achieved. However, a shift towards lower angles is observed,

indicating an increase in the interlayer gallery, associated with a predominantly intercalated morphology.

Regarding the samples containing HNTs, it is possible to observe the most intense diffraction peak of HNT (001) at 2θ = 11.95° (corresponding to a basal spacing of 0.74 nm). No changes were observed in the shape or position of this peak in the PHBV-HNT nanocomposites. This result indicates that after blending no changes occur in the tubular structure of the primary particles of halloysite. The addition of chain extender does not affect either the crystalline structure of PHBV or the interlayer distance of the clay.

Thermal characterization

TGA experiments were carried out to investigate the effect of the addition of clay and chain extenders on the thermal stability of PHBV. Figure 4 plots the mass loss and the DTG versus temperature for the neat PHBV and PHBV nanocomposites, while Table I summarizes the values of $T_{5\%}$ and T_d for all the samples studied.

The thermal degradation of neat PHBV consists of a single weight loss step between 240 and 320 °C (Table I), according to the random chain scission reaction.[42] The maximum rate of mass loss takes place at 285 °C and $T_{5\%}$ (the temperature at which the mass loss is 5%) at 268 °C. Some differences in the thermal degradation of PHBV are observed with the incorporation of the clays.

Once the degradation has begun, the reaction rate clearly decreases with respect to the pure polymer, showing a higher T_d with respect PHBV, from 285 to 288 and 294 °C for C30B and HNT, respectively. This behavior can be explained by the fact that the clays, together with the solid degradation products, generate a dense coating that hinders the development

of further degradation by opposing a strong mass transport resistance to the volatile agents involved in the reaction, resulting in a decrease of the degradation kinetics.[43] These results are in agreement with the work reported by Bittmann et al. and Bruzaud et al. in which different nanoclays (non modified montmorillonite, bentonite and Cloisite®15A) showed similar trends in thermogravimetric analysis.

With respect to the presence of HNT in the PHBV matrix, it also increases the thermal stability of PHBV, with a rise in $T_{5\%}$ from 268 to 277 °C. On the other hand, the sample containing C30B exhibits a degradation onset similar to that of the neat PHBV, as derived from the $T_{5\%}$. In other works it has been reported a decrease on the $T_{5\%}$ with PHBV/C30B composites. [12,44–46] This behaviour is generally attributed to the clay modifiers that may have a catalytic action in the degradation of PHBV.[15] In our case, the opposed phenomena of stabilizing and catalizing the degradation yield in no significant variation on the $T_{5\%}$. Additionally, it has been suggested that the water adsorbed to the clays may contribute to accelerate the degradation rate in clay/PHBV composites, hindering the thermal stabilizing effect of the clays. [12] The thermal history and severity of processing conditions, especially with clays, may have also an influence in the degradation kinetics of the samples. [47]

The effect of the addition of TNPP to both neat PHBV and the nanocomposites on the thermal degradation behavior can be seen in Fig. 5. As expected, the presence of the chain extender improves the thermal stability of PHBV, as derived from the increases of $T_{5\%}$ and T_d by 8 and 10 °C, respectively. This issue is of special relevance since during food packaging operations there are many thermic cycles (film processing, stretching, thermoforming, hot sealing, etc) where some local thermal degradation can occur, being the products of such degradation susceptible to migrate towards the content of the package. [48]

The addition of TNPP to the sample containing the C30B clay revealed a shift of the curve towards higher temperatures, thus showing an increase of ca. 5 °C in both $T_{5\%}$ and Td with respect to that without the chain extender. These results would indicate that the addition of TNPP to PHBV/clay nanocomposites may improve their thermal resistance. On the other hand, the PHBV-HNT-TNPP sample does not show relevant changes in thermal degradation when compared with that without the chain extender. This lack of a synergetic effect between the TNPP and the halloysite could be explained by the fact that, as inferred from the SEM analysis, the TNPP is partially adsorbed over the surface of the clay, thus decreasing the chain extender activity.

DSC experiments were conducted in order to evaluate the influence of the addition of the nanoclays and chain extender on the crystallization characteristics of PHBV. Table 1 summarizes the crystallization and melting temperatures, crystallization enthalpy, and degree of crystallinity of all the samples studied in this work.

After analyzing the resulting DSC parameters, it can be appreciated that the crystallization temperature (T_c) of PHBV was not significantly modified when the nanoclays were incorporated. The degree of crystallinity (X_c) also remained similar, at around 66%, in agreement with other works and a similar processing history.[11,37] On the other hand, during the second heating scan it could be observed that the peak melting temperature (T_m) decreased by about 5 °C with C30B and 3ºC with HNT. These results suggest that nanoclays make the formation of thick lamella more difficult than neat PHBV, being more pronounced in the case of C30B.

When TNPP was added to PHBV, a small decrease on T_m is detected, pointing to some reduction in lamellar thickness; but when it is combined with C30B or HNT, the T_m increases

slightly with respect to the composites without TNPP. In any case, it is consideded that the variations in T_c, X_c and T_m shown are not of great significance, indicating that 1%wt of TNPP has little interference with the crystallization processes of PHBV.

Mechanical properties

Tensile tests to rupture were conducted on hot-pressed films for all the samples studied. Figures 6a and 6b plot the evolution of the Young's modulus and the tensile strength of the PHBV with the addition of the clays and the TNPP. The Young's modulus of PHBV showed significant increases of 69 and 80% with the addition of 5 wt% C30B and HNT, respectively. Regarding the tensile strength, increases of 12 and 34% were detected with the addition of both C30B and HNT. This enhancement in stiffness and tensile strength of PHBV/clay nanocomposites was at the expense of a significant reduction in the elongation at break (see Fig. 6c). In this sense, drops of 63 and 50% in the elongation at break can be observed with the addition of 5 wt% C30B and HNTs, respectively. Altogether these results show a clear reinforcing effect of the nanoclays on the PHBV matrix. These results are in agreement with other works. [12,44,46,49,50]

The addition of TNPP to the neat PHBV resulted in increases in the Young's modulus (44%) and the tensile strength (30%), similar to those obtained by the addition of nanoclays. Some studies with PCL and PLA showed that the increase in the Young's modulus and tensile strength with the addition of chain extenders could be ascribed to the increased molecular weight, together with the formation of a long chain branching structure.[25,51,52] On the other hand, the strain at break of PHBV containing the chain extender decreases compared to that of the original polymer. This can be explained by the fact that the increased density of

entanglements of the polymer structure with the long chain branching hinders the slipping of the polymer chains.[25,53,54]

Regarding the combined effect of the nanoclays with the TNPP on the mechanical properties of PHBV, surprisingly, no relevant changes were observed when TNPP was added to PHBV-C30B nanocomposites. However, an increase in elongation at break and a decreased Young's modulus and tensile strength with respect to the PHBV-HNT nanocomposite were observed.

Such different behavior could be attributed to the effect of partial absorption of TNPP on the clay surface discussed previously on the morphological and thermal stability analysis.

Taking this into account, the the mechanical properties of the PHBV/HNT/TNPP nanocomposites are similar to those of PHBV/TNPP, since the reinforcement of the HNT are limited by the partial absorption of the TNPP. These results suggest that the properties of PHBV/HNT nanocomposites could be improved by modifying the mixing procedures, in order to minimize the absorption of TNPP on the active surface of HNT.

The improvement on mechanical properties opens up the possibility to reduce thickness in food packaging products, thus decreasing the overall costs while preserving the other characteristics of the package. It is worthwhile to recall that this type of industry uses large amounts of raw material and a reduction of 5-10% in volume may have a huge impact of the final economic and environmental balance of the package.

CONCLUSIONS

PHBV nanocomposites with two different clays (Cloisite®30B and halloysite nanotubes) and a chain extender (TNPP) were successfully obtained by melt blending. Favorable morphologies were achieved during processing for both nanoadditives (i.e. predominantly

intercalated/exfoliated morphology in the PHBV-C30B and good distribution of halloysite nanotubes within the polymer matrix) as derived from TEM, SEM, and WAXS experiments.

The properties of such compounds are characterized by an increase in the thermal stability of PHBV through incorporation of TNPP as a chain extender and/or HNTs. The addition of C30B only improves the thermal stability by decreasing the degradation rate. On the other hand, the addition of chain extenders or clays within the range studied did not significantly alter the crystallization temperature and overall crystallinity, and there was a slightly variation in the peak melting temperature.

Regarding the mechanical properties, the nanocomposites prepared with C30B and HNT revealed a reinforced behavior when compared to the neat PHBV, with higher stiffness and tensile strength and a decreased elongation at break. However, no relevant changes were observed when TNPP was added to PHBV nanocomposites.

ACKNOWLEDGMENTS

Financial support for this research from Ministerio de Economía y Competitividad (project MAT2012-38947-C02-01), Generalitat Valenciana (GV/2014/123), and Pla de Promoció de la Investigació de la Universitat Jaume I (PREDOC/2012/32) is gratefully acknowledged. The authors are also grateful to Raquel Oliver and José Ortega for experimental support.

REFERENCES

1. Lenz, R. W.; Marchessault, R. H. *Biomacromolecules* **2005**, *6*, 1–8.

2. Chea, V.; Angellier-Coussy, H.; Peyron, S.; Kemmer, D.; Gontard, N. *J. Appl. Polym. Sci.* **2015**, Article in press.

3. Bucci, D. Z.; Tavares, L. B. B.; Sell, I. *Polym. Test.* **2005**, *24*, 564–571.

4. Cava, D.; Gimenez, E.; Gavara, R.; Lagaron, J. M. *J. Plast. Film Sheeting* **2006**, *22*, 265–274.

5. Lagaron, J. M.; Lopez-Rubio, A. *Trends Food Sci. Technol.* **2011**, *22*, 611–617.

6. Rhim, J.-W.; Park, H.-M.; Ha, C.-S. *Prog. Polym. Sci.* **2013**, *38*, 1629–1652.

7. Lagarón, J. M.; Cabedo, L.; Cava, D.; Feijoo, J. L.; Gavara, R.; Gimenez, E. *Food Addit. Contam.* **2005**, *22*, 994–998.

8. Bordes, P.; Pollet, E.; Averous, L. *Prog. Polym. Sci.* **2009**, *34*, 125–155.

9. Sanchez-Garcia, M. D.; Lagaron, J. M. *J. Appl. Polym. Sci.* **2010**, *118*, 188–199.

10. Reddy, M. M.; Vivekanandhan, S.; Misra, M.; Bhatia, S. K.; Mohanty, A. K. *Prog. Polym. Sci.* **2013**, *38*, 1653–1689.

11. Crétois, R.; Follain, N.; Dargent, E.; Soulestin, J.; Bourbigot, S.; Marais, S.; Lebrun, L. *J. Memb. Sci.* **2014**, *467*, 56–66.

12. Carli, L. N.; Crespo, J. S.; Mauler, R. S. *Compos. Part A Appl. Sci. Manuf.* **2011**, *42*, 1601–1608.

13. Cabedo, L.; Plackett, D.; Giménez, E.; Lagarón, J. M. *J. Appl. Polym. Sci.* **2009**, *112*, 3669–3676.

14. Bordes, P.; Hablot, E.; Pollet, E.; Avérous, L. *Polym. Degrad. Stab.* **2009**, *94*, 789–796.

15. Bellucci, F.; Camino, G.; Frache, A.; Sarra, A. *Polym. Degrad. Stab.* **2007**, *92*, 425–436.

16. Hablot, E.; Bordes, P.; Pollet, E.; Avérous, L. *Polym. Degrad. Stab.* **2008**, *93*, 413–421.

17. Shi, Y.-F.; Tian, Z.; Zhang, Y.; Shen, H.-B.; Jia, N.-Q. *Nanoscale Res. Lett.* **2011**, *6*, 608–614.

18. Guimarães, L.; Enyashin, A. N.; Seifert, G.; Duarte, H. A. *J. Phys. Chem. C* **2010**, *114*, 11358–11363.

19. Joussein, E.; Petit, S.; Churchman, J.; Theng, B.; Righi, D.; Delvaux, B. *Clay Miner.* **2005**, *40*, 383–426.

20. Rawtani, D.; Agrawal, Y. *Rev. Adv. Mater. Sci.* **2012**, *30*, 282–295.

21. Russo, P.; Vetrano, B.; Acierno, D.; Mauro, M. *Polym. Compos.* **2013**, *34*, 1460–1470.

22. Javadi, A.; Srithep, Y.; Pilla, S. *Polym. Eng. Sci.* **2011**, *51*, 1815–1826.

23. Liu, Q.-S.; Zhu, M.-F.; Wu, W.-H.; Qin, Z.-Y. *Polym. Degrad. Stab.* **2009**, *94*, 18–24.

24. Najafi, N.; Heuzey, M. C.; Carreau, P. J. *Polym. Eng. Sci.* **2013**, *53*, 1053–1064.

25. Najafi, N.; Heuzey, M. C.; Carreau, P. J.; Wood-Adams, P. M. *Polym. Degrad. Stab.* **2012**, *97*, 554–565.

26. Najafi, N.; Heuzey, M. C.; Carreau, P. J. *Compos. Sci. Technol.* **2012**, *72*, 608–615.

27. Al-Itry, R.; Lamnawar, K.; Maazouz, A. *Polym. Degrad. Stab.* **2012**, *97*, 1898–1914.

28. Meng, Q.; Heuzey, M.-C.; Carreau, P. J. *Polym. Degrad. Stab.* **2012**, *97*, 2010–2020.

29. Rytlewski, P.; Żenkiewicz, M.; Malinowski, R. *Int. Polym. Process.* **2011**, *26*, 580–586.

30. Burlet, J.; Heuzey, M. C.; Dubois, C.; Wood-Adams, P.; Brisson, J. *Annu. Tech. Conf. - ANTEC, Conf. Proc.* **2005**, *3*, 281–285.

31. Cicero, J. A.; Dorgan, J. R.; Dec, S. F.; Knauss, D. M. *Polym. Degrad. Stab.* **2002**, *78*, 95–105.

32. Lehermeier, H. J.; Dorgan, J. R. *Polym. Eng. Sci.* **2001**, *41*, 2172–2184.

33. D'Haene, P.; Remsen, E. E.; Asrar, J. *Macromolecules* **1999**, *32*, 5229–5235.

34. Bikiaris, D.; Karayannidis, G. *J. Polym. Sci. Part A Polym. Chem.* **1996**, *34*, 1337–1342.

35. D'Haene, P.; Remsen, E. E.; Asrar, J. *Macromolecules* **1999**, *32*, 5229–5235.

36. Fei, B.; Chen, C.; Chen, S.; Peng, S.; Zhuang, Y.; An, Y.; Dong, L. *Polym. Int.* **2004**, *53*, 937–943.

37. Duangphet, S.; Szegda, D.; Song, J.; Tarverdi, K. *J. Polym. Environ.* **2013**, *22*, 1–8.

38. Fensterheim, R. J. In *Society of Plastics Engineers - International Polyolefins Conference - FLEXPACKCON 2008*; **2008**; Vol. 2, pp. 643–650.

39. Savenkova, L.; Gercberga, Z.; Bibers, I.; Kalnin, M. *Process Biochem.* **2000**, *36*, 445–450.

40. Heo, K.; Yoon, J.; Jin, K.; Jin, S. *J. Phys. Chem.* **2008**, *112*, 4571–4582.

41. Alata, H.; Aoyama, T.; Inoue, Y. *Macromolecules* **2007**, *40*, 4546–4551.

42. Grassie, N.; Murray, E. J.; Holmes, P. A. *Polym. Degrad. Stab.* **1984**, *6*, 127–134.

43. Du, M.; Guo, B.; Jia, D. *Eur. Polym. J.* **2006**, *42*, 1362–1369.

44. Carli, L. N.; Daitx, T. S.; Soares, G. V.; Crespo, J. S.; Mauler, R. S. *Appl. Clay Sci.* **2014**, *87*, 311–319.

45. Wang, S.; Song, C.; Chen, G.; Guo, T.; Liu, J.; Zhang, B.; Takeuchi, S. *Polym. Degrad. Stab.* **2005**, *87*, 69–76.

46. Bordes, P.; Pollet, E.; Bourbigot, S.; Avérous, L. *Macromol. Chem. Phys.* **2008**, *209*, 1473–1484.

47. Zaverl, M.; Seydibeyoğlu, M. Ö.; Misra, M.; Mohanty, A. *J. Appl. Polym. Sci.* **2012**, *125*, E324–E331.

48. Incarnato, L.; Di Maio, L.; Acierno, D.; Denaro, M.; Arrivabene, L. *Food Addit. Contam.* **1998**, *15*, 195–202.

49. Bruzaud, S.; Bourmaud, A. *Polym. Test.* **2007**, *26*, 652–659.

50. Chen, G. X.; Hao, G. J.; Guo, T. Y.; Song, M. D.; Zhang, B. H. *J. Appl. Polym. Sci.* **2004**, *93*, 655–661.

51. Liu, J.; Lou, L.; Yu, W.; Liao, R.; Li, R.; Zhou, C. *Polymer (Guildf).* **2010**, *51*, 5186–5197.

52. Grosvenor, M. *Int. J. Pharm.* **1996**, *135*, 103–109.

53. Kennedy, M. A.; Peacock, A. J.; Mandelkern, L. *Macromolecules* **1994**, *27*, 5297–5310.

54. Lin, G.; Shih, H. *Polym. Eng. Sci.* **2002**, *42*, 2213–2221.

Figure Captions:

Fig 1: TEM micrograph of (a) PHBV-C30B and (b) PHBV-HNT

Fig 2: SEM images of the fracture surface of a) PHBV-C30B, b) PHBV-C30B-TNPP, c) PHBV-HNT, and d) PHBV-HNT-TNPP

Fig 3: WAXS pattern of neat PHBV, PHBV-C30B, and PHBV-HNT nanocomposites

Fig 4: TGA and DTG curves of PHBV/clay nanocomposites

Fig 5: TGA and DTG curves of PHBV and PHBV/clay nanocomposites with and without chain extender

Fig 6: Young's modulus, tensile strength, and elongation at break of PHBV/clay nanocomposites with and without chain extender

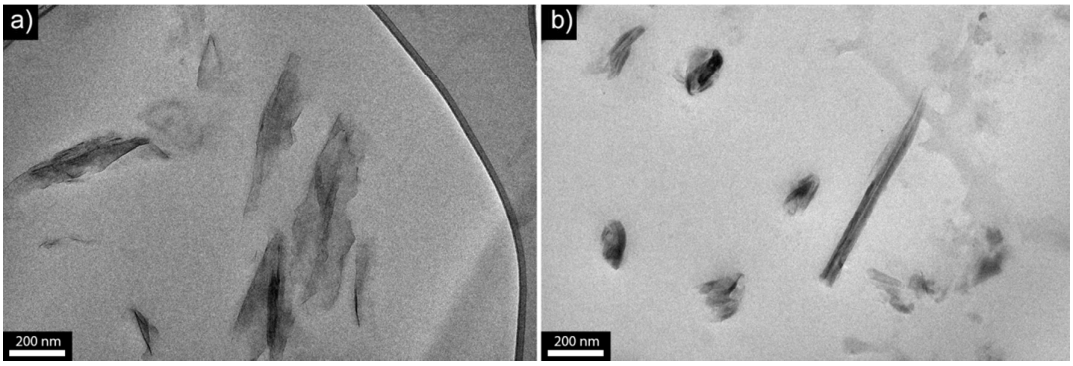

FIGURE 1: González-Ausejo et al.

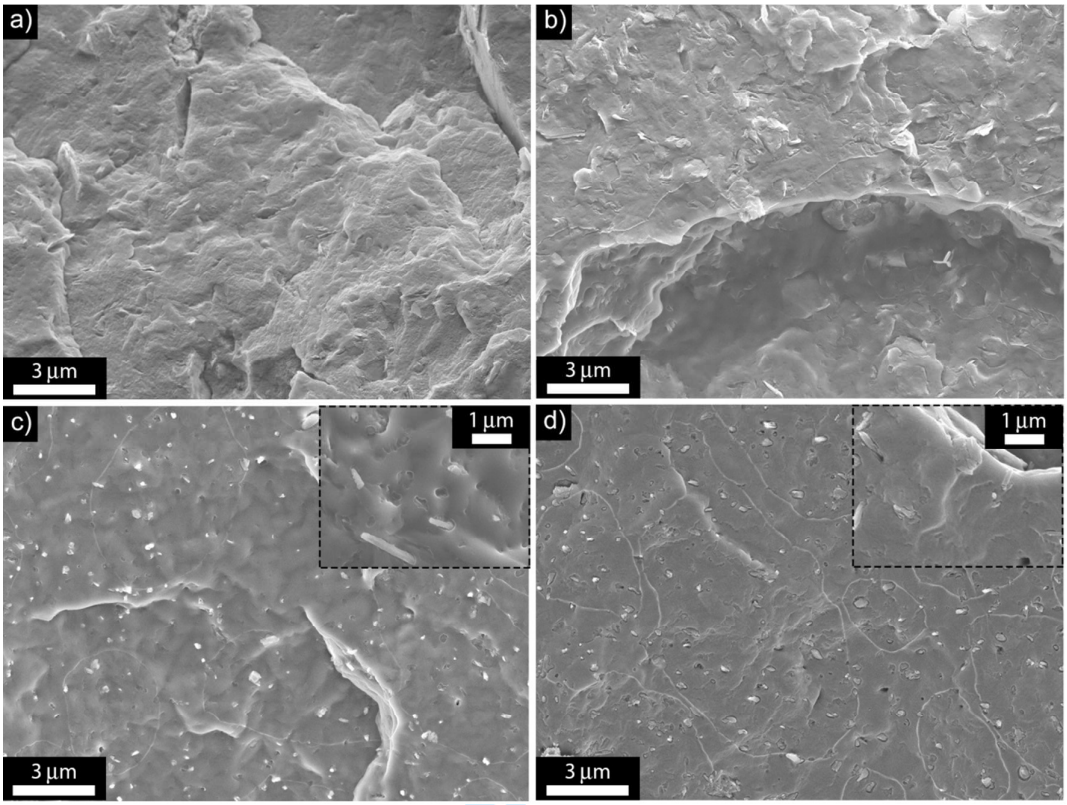

FIGURE 2: González-Ausejo et al.

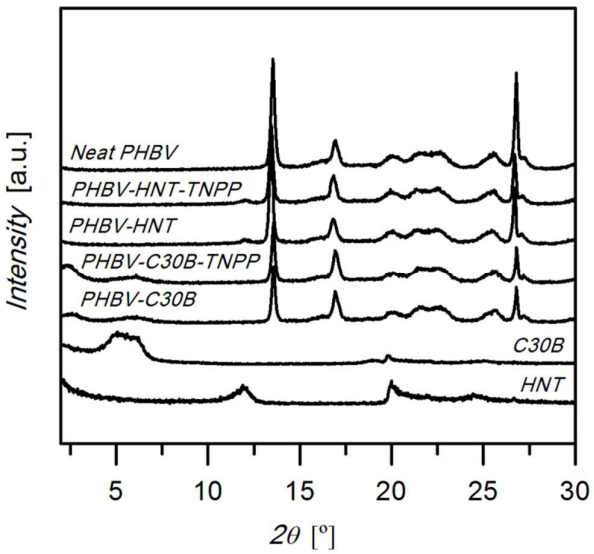

FIGURE 3: González-Ausejo et al.

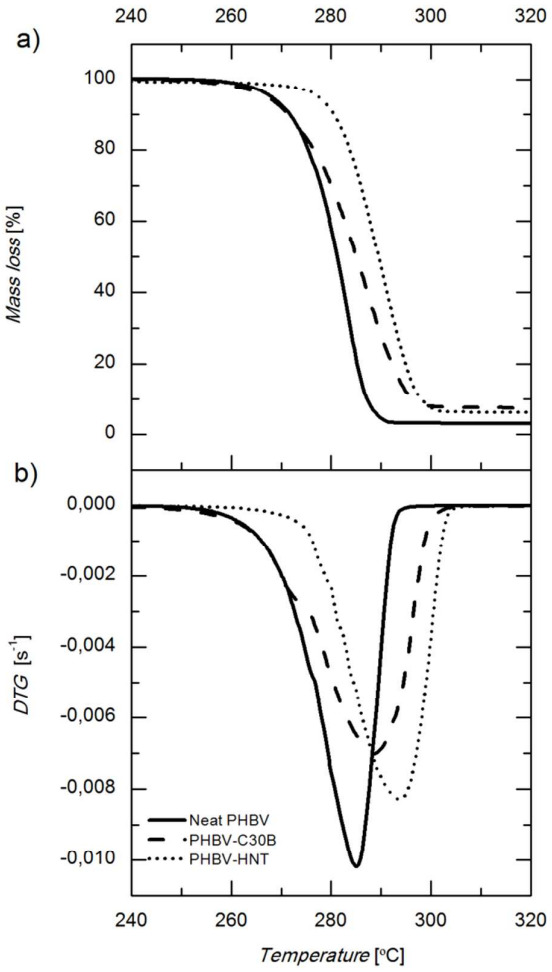

FIGURE 4: González-Ausejo et al.

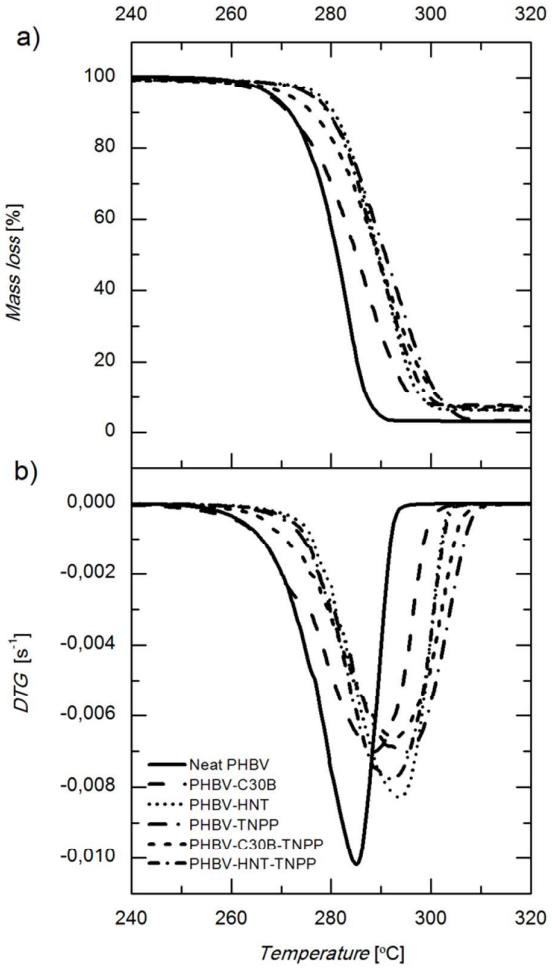

FIGURE 5: González-Ausejo et al.

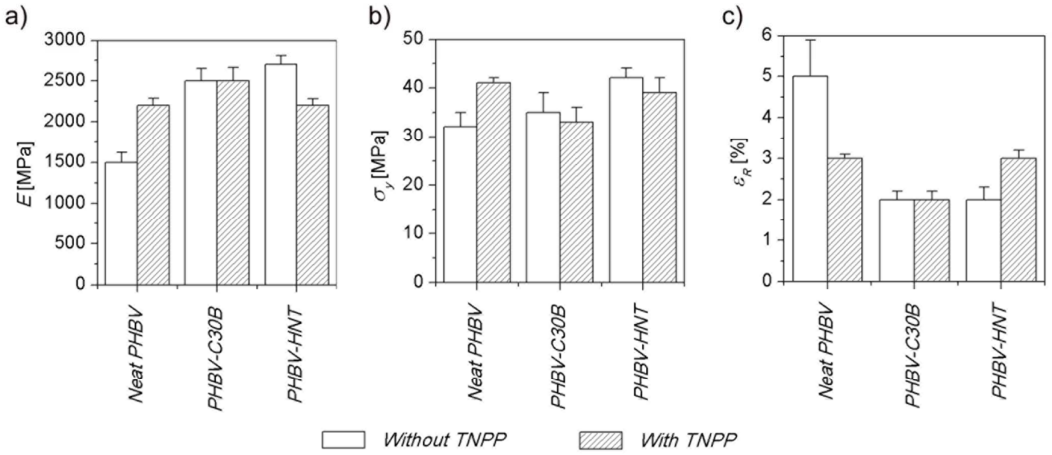

FIGURE 6: González-Ausejo et al.

Table Captions:

Table 1: DSC and TGA data of the samples studied.

Table 2: Mechanical properties of PHBV and its nanocomposites

TABLE 1: González-Ausejo et al.

	T_c (ºC)	T_m (ºC)	ΔH_c (J/g)	X_c (%)	$T_{5\%}$ (ºC)	T_d (ºC)
Neat PHBV	115	169	96	66	268	285
PHBV-C30B	115	164	96	66	267	288
PHBV-HNT	115	166	98	67	277	294
PHBV-TNPP	113	166	97	66	276	295
PHBV-C30B-TNPP	114	165	100	68	272	293
PHBV-HNT-TNPP	115	169	97	66	277	292

TABLE 2: González-Ausejo et al.

	E (MPa)	σ_y (MPa)	ε_R (%)
Neat PHBV	1500±120	32±3	5±0,9
PHBV-C30B	2500±150	35±4	2±0,2
PHBV-HNT	2700±115	42±2	2±0,3
PHBV-TNPP	2200±90	41±1	3±0,1
PHBV-C30B-TNPP	2500±160	33±3	2±0,2
PHBV-HNT-TNPP	2200±80	39±3	3±0,2